Science of the Total Environment 878 (2023) 162895

Contents lists available at ScienceDirect

Science of the Total Environment

journal homepage: www.elsevier.com/locate/scitotenv

Methane and carbon dioxide fluxes at high spatiotemporal resolution from a small temperate lake

Jonas Stage Sø [a,*], Kaj Sand-Jensen [b], Kenneth Thorø Martinsen [b], Emma Polauke [a], Johan Emil Kjær [b], Kasper Reitzel [a], Theis Kragh [a]

[a] University of Southern Denmark, Campusvej 55, 5230 Odense M, Denmark
[b] University of Copenhagen, Universitetsparken 4, 3 floor, 2100 Copenhagen, Denmark

HIGHLIGHTS

- A new method for measuring CH_4 and CO_2 fluxes at high spatio-temporal resolution
- Methane diffusion and ebullition showed extensive spatio-temporal variability.
- 476 ebullitive events occurred among the 1.9 million CH_4 measurements.
- Ebullitive CH_4 fluxes were highest from the deeper parts of the lake.
- Methane ebullition was four times higher than diffusive CH_4 fluxes.

GRAPHICAL ABSTRACT

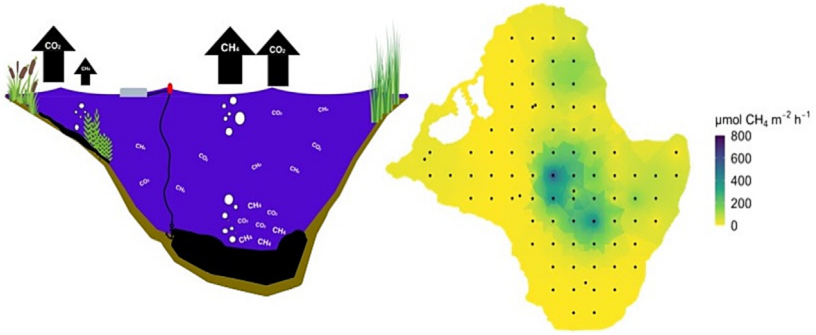

ARTICLE INFO

Editor: José Virgílio Cruz

Keywords:
Lake greenhouse gas emissions
Climate change
Automated floating chambers
CH_4 fluxes
CO_2 fluxes

ABSTRACT

Lakes are hotspots for CH_4 and CO_2 effluxes, but their magnitude and underlying drivers are still uncertain due to high spatiotemporal variation within and between lakes. We measured CH_4 and CO_2 fluxes at high temporal (hourly) and spatial resolution (approx. 13 m) using 24 automatic floating chambers equipped with continuously recording sensors that enabled the determination of diffusive and ebullitive gas fluxes. Additionally, we measured potential drivers such as weather patterns, water temperature, and O_2 above the sediment. During five days in autumn 2021, we conducted measurements at 88 sites in a small, shallow eutrophic Danish Lake. CH_4 ebullition was intense (mean 54.8 μmol m^{-2} h^{-1}) and showed pronounced spatiotemporal variation. Ebullition rates were highest in deeper, hypoxic water (5–7 m). Diffusive CH_4 fluxes were 4-fold lower (mean 15.0 μmol m^{-2} h^{-1}) and spatially less variable than ebullitive fluxes, and significantly lower above hard sediments and submerged macrophyte stands. CO_2 concentration in surface waters was permanently supersaturated at the mid-lake station, and diffusive fluxes (mean 919 μmol m^{-2} h^{-1}) tended to be higher from deeper waters and increased with wind speed. To obtain mean whole-lake fluxes within an uncertainty of 20 %, we estimated that 72 sites for CH_4 ebullition, 39 sites for diffusive CH4 fluxes and 27 sites for diffusive CO_2 fluxes would be required. Thus, accurate whole-lake quantification of the dominant ebullitive CH_4 flux requires simultaneous operation of many automated floating chambers. High spatiotemporal variability challenges the identification of essential drivers and current methods for upscaling lake CH_4 and CO_2 fluxes. We successfully overcame this challenge by using automatic floating chambers, which offer continuous CH_4 and CO_2 flux measurements at high temporal resolution and, thus, are an improvement over existing approaches.

* Corresponding author.
E-mail address: jonassoe@biology.sdu.dk (J.S. Sø).

http://dx.doi.org/10.1016/j.scitotenv.2023.162895
Received 2 September 2022; Received in revised form 9 March 2023; Accepted 12 March 2023
Available online 22 March 2023

1. Introduction

Atmospheric concentrations of methane (CH_4) and carbon dioxide (CO_2) have increased profoundly over the past 100 years (European Environment Agency, 2019). Greenhouse gas fluxes from lakes and ponds have recently received more attention due to high fluxes of CH_4 and CO_2. Rosentreter et al. (2021) found that aquatic ecosystems emit more than half of the global CH_4 emissions; lakes and reservoirs showing high median values of 35–72 μmol m^{-2} h^{-1}. Sieczko et al. (2020) found CH_4 fluxes reaching approximately 14 μmol m^{-2} h^{-1} in sub-arctic Sweden, while Bastviken et al. (2004) in temperate lakes found mean ebullitive and diffusive CH_4 fluxes of 85 and 27 μmol m^{-2} h^{-1}, respectively. The reported CH_4 effluxes are highly variable, resulting in large uncertainties in global flux estimates (Bastviken et al., 2004). The ambiguity in reported CH_4 fluxes can be attributed partly to the high expense associated with measuring CH_4 at high spatial and temporal resolution (Bastviken et al., 2004). Fortunately, newly developed cost-efficient sensors installed in floating chambers can measure CH_4 and CO_2 fluxes continuously (Bastviken et al., 2020).

Most attempts to measure CH_4 have been based on a small number of samples within lakes ($n < 15$), hampering evaluation of spatiotemporal variations and whole-lake fluxes, while a few comprehensive studies (e.g., Keller and Stallard (1994) ($n = 362$); Sieczko et al. (2020) ($n = 134$)) investigated depth patterns in CH_4 ebullition and diel changes of CH_4 fluxes. To our knowledge, no study to date has offered a comprehensive analysis of spatial differences in CH_4 fluxes within a lake, whereas spatial differences in CO_2 fluxes within lakes have received more attention (Andrade et al., 2016). Once these differences have been identified, it becomes possible to identify their controlling factors and ensure accurate determination of the flux for whole lakes.

Differences in CH_4 and CO_2 fluxes within and among lakes have mostly been attributed to nutrient status, dissolved organic carbon (DOC) concentrations, and lake size and morphometry (Bastviken et al., 2004; Keller and Stallard, 1994; Sieczko et al., 2020). Additionally, hydrothermal-magmatic flow and geogenic sources may also influence CH_4 and CO_2 fluxes, but this is only profound in volcanic areas (Tassi et al., 2018), while hydrothermal-magmatic flow does not exist in the lake and region studied here (Lake Lyng, Denmark). Furthermore, groundwater inputs to a lake can contain high concentrations of carbon (C), promoting increased CH_4 and CO_2 formation and thereby emissions (Striegl and Michmerhuizen, 1998). Additionally, stratification of lake water can reduce emission rates as bottom water with high concentrations of CH_4 and CO_2 does not reach the water-air interface, simultaneously, a buildup of CH_4 oxidizing bacteria at the oxic-anoxic layer is formed, causing reduced CH_4 concentrations reaching the water-air interface (Bastviken, 2009; Tassi et al., 2018). Higher lake trophic status and DOC concentration work as proxies for the productivity and external input to lakes, causing a positive relationship between lake productivity and CH_4 fluxes due to higher sedimentation and mineralization of organic matter in sediments with overlying anoxic waters (Bastviken et al., 2004). Furthermore, a positive relationship between lake productivity and the duration of summer stratification would increase the areal extent of anoxic sediments, thus promoting CH_4 formation (Bastviken et al., 2004). A high proportion of labile organic carbon increases the formation of acetate and hydrogen, fueling CH_4 production under anoxia (Fenchel et al., 2012). High input of allochthonous carbon is also known to increase CO_2 efflux due to stimulated heterotrophic degradation and respiration (Bastviken et al., 2004). Therefore, we expect that lake sediment's organic content links directly to CH_4 production. However, sediment organic matter content in lakes can be highly variable and time-consuming to measure. As an alternative, we used sonar imaging as a relatively fast assessment of sediment hardness usually correlated with sediment organic matter content (Kragh et al., 2017; Sø et al., 2021).

Lake morphometry and wind exposure affect both the ebullitive and diffusive CH_4 fluxes as well as CH_4 retention and oxidation in the water (Bastviken, 2009). CH4 flux has been shown to decrease with lake area, possibly due to a lower input of allochthonous organic carbon and nutrients relative to lake volume (Bastviken et al., 2004). Moreover, a greater lake size increases wind exposure and gas transfer velocity across the water–air interface (Vachon and Prairie, 2013). Wind-induced turbulence and water depth influence shear stress, oxygen influx to the sediment, and likely the CH_4 production and release (Bastviken et al., 2004). A deeper water column can also increase the loss of CH_4 from bubbles during the passage from the sediment to the water surface, thereby reducing the flux of CH_4 to the atmosphere (Langenegger et al., 2019).

It should be easier to quantify the CO_2 flux than the CH_4 flux because of the higher solubility of CO_2 compared to CH_4, resulting in the vast majority of CO_2 exchange occurring by diffusion across the water surface (Enick and Klara, 1990) in contrast to CH_4, which may show large effluxes by ebullition (Bastviken et al., 2004). Dissolved gases are distributed by advective and convective mixing, which tends to reduce spatial variations of concentrations (Boehrer and Schultze, 2008). Both CO_2 and CH_4 are exchanged across the water-air interface by diffusion according to the product of the partial pressure gradient and the gas transfer velocity (Rosentreter et al., 2021). Diel changes of the CO_2 partial pressure gradient may be substantial due to daytime CO_2 consumption in gross primary production, while CO_2 release by ecosystem respiration continues day and night (Natchimuthu et al., 2014; van Bergen et al., 2019). Diel variation of the gas transfer velocity may also be prominent, as near-surface turbulence is driven by wind shear and convection (Andersen et al., 2017). Moreover, local sheltering and differential heating and cooling may result in a spatial variation of the partial pressure gradients of both gases (Schilder et al., 2013) and the gas transfer velocity (Sand-Jensen et al., 2021). Thus, low horizontal mixing and different metabolic intensity between littoral and pelagic habitats may generate spatial variability of diffusive gas fluxes. The uncertainties in emissions are noticeable in reported values, Rosentreter et al. (2021) review estimated that more than half of global CH_4 emissions derives from aquatic systems, with lakes between 1–10 and 10–100 ha having average (± 95 % C.I.) CH_4 emissions of 255 ± 102 and 162 ± 98 μmol m^{-2} h^{-1}. However, CH_4 flux has been measured primarily during daytime, limiting the insight into diel variability (Sieczko et al., 2020). Existing studies show contradictory results regarding whether daytime or nighttime CH_4 fluxes are highest, and underlying drivers have not been identified with certainty (Podgrajsek et al., 2014; Sieczko et al., 2020).

Our overall objective was to measure CH_4 and CO_2 fluxes at high spatiotemporal resolution from a 10-ha eutrophic Danish lake and evaluate the environmental drivers explaining the variance in the fluxes. We measured environmental variables and applied CH_4 and CO_2 sensors mounted in floating chambers that automatically replenished headspace air. The chambers were deployed for five consecutive days and were moved to a new position every day, creating a spatial grid of one-day measurements. In addition, five chambers were kept in the same position to measure day-to day variations in gas fluxes. We hypothesized that: 1) spatial variability of ebullitive CH_4 fluxes is higher than for diffusive CH_4 and CO_2 fluxes due to the mixing of dissolved gases throughout the surface waters; 2) temporal variability of CH_4 emissions is low, though higher during daytime when wind and sediment shear stress may increase relative to nighttime; and 3) the main underlying drivers of variable CH_4 fluxes would be sediment hardness and oxygen availability at the sediment surface both being dependent on site location and water depth.

2. Materials and methods

This study was conducted in Lake Lyng, a small (10 ha) softwater (alkalinity 0.9 meq l^{-1}) shallow lake (mean depth 2.4 m, max. 7.6 m) located near the town of Silkeborg, Denmark (56.158668, 9.544308, Fig. 1). Lake Lyng has a small catchment of 0.56 km^2 of which 45 % are residential areas and a water residence time of approximately 1.4 years. The water entering the lake is primarily by surface runoff and probably groundwater input, as the lake has no distinct inlet and only a small outlet (Skovgaard and Carl, 2018). During the early autumn measuring period there was no surface water inlet or outlet. As the lake received untreated wastewater from 1889 until the mid-1950s, it became hypertrophic (> 200 μg total-P l^{-1}; Bundgaard et al. (2002)). Nutrient concentrations decreased after

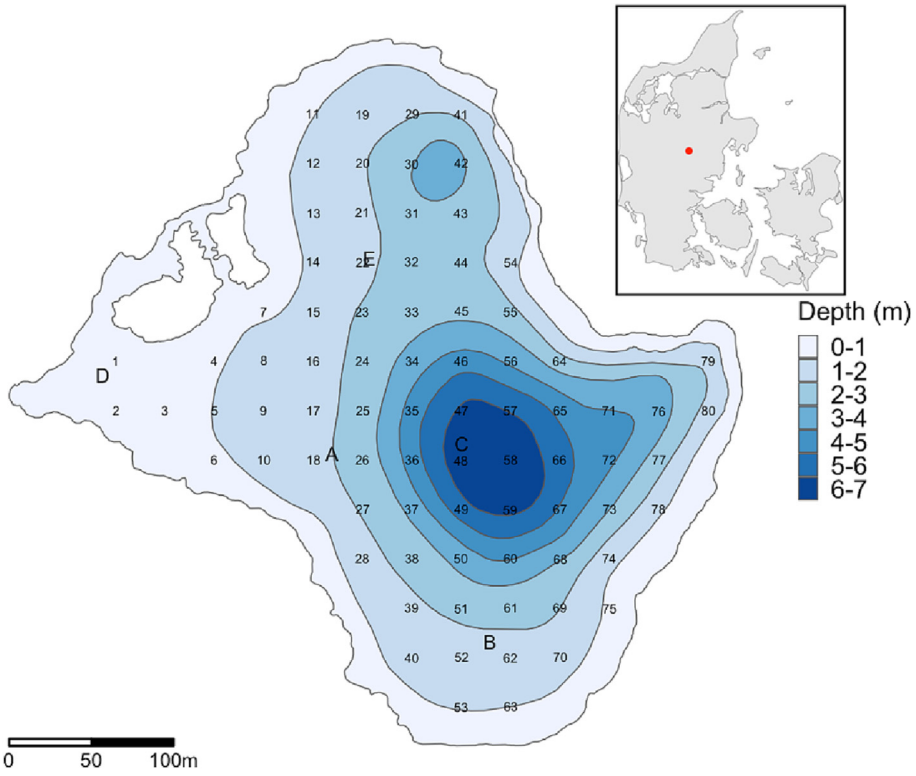

Fig. 1. Bathymetric map of Lake Lyng and stations where environmental variables and gas fluxes were measured. Temporary stations are shown as numbers (1–80) and permanent stations as letters (A–E). The inset map shows the location of Lake Lyng in Denmark.

sewage input stopped, and average summer concentrations in 2016 were 37 μmol total-N l^{-1} and 2 μmol total-P l^{-1} (Skovgaard and Carl, 2018).

2.1. Environmental conditions

We continuously measured GHG fluxes from floating chambers and multiple environmental variables for five days from 27 September – 1 October 2021. From a buoy at the deepest point in the lake (7.6 m), we measured photosynthetically active radiation (PAR; HOBO S-LIA-M003, Onset, USA), wind speed, gust and direction (HOBO S-WSET-A), and temperature through the water column (HOBO UA-002-64) at 1 m intervals. Air temperature, barometric pressure, and relative humidity were measured every minute at a public weather station (Davis Vantage Pro2) located 3.5 km from the lake (Jessen, 2021). Oxygen was measured below each GHG chamber with a sensor (MiniDOT, PME, USA) suspended 0.5 m above the sediment surface. Alkalinity was measured on duplicate surface samples collected during the measurement period and analyzed by acidimetric titration (Gran, 1952). Water CO_2 concentration was calculated from measurements of pH, water temperature, and alkalinity (Hofmann et al., 2010).

Water depth, sediment hardness, and submerged aquatic plant coverage were determined across the lake using sonar (Lowrance HDS-16 Live equipped with a Lowrance Hybrid Dual Imaging (HDI) Skimmer Transducer and Active Imaging 3-in-1 Transducer). Sonar data were collected in September 2021 and analyzed as described in Kragh et al. (2017). In short, lake isobaths and maps of sediment hardness were calculated using Reefmaster 2.0 (Reefmaster Software Limited) with the bottom composition module and a maximum interpolation between paths of 15 m, while data points were recorded in one-meter intervals. Aquatic plant coverage and species separation were assessed using sidescan imagery, which was possible due to the low aquatic plant biodiversity and easily distinguishable signals of the species. When aquatic plants were present on the sidescan images a plant sample was collected for species identification. Two species of aquatic plants (*Potamogeton crispus* and *Ceratophyllum demersum*) and macroalgae were present and distinguishable on the sidescan imagery. Only *P. crispus* was rooted in the sediment and was included in the estimation of plant coverage.

CH_4 input via groundwater was estimated to explore whether input of CH_4-rich groundwater could account for the observed CH_4 fluxes. The calculations were made using 395 mm of yearly groundwater input relative to surface area, representing the mean value of the region (Sand-Jensen et al., 2006), multiplied by the effective catchment area of the lake. Much of the catchment consists of residential areas which are sewered and do not contribute groundwater to the lake. Concentrations of CH_4 and CO_2 in groundwater wells in the vicinity of the lake from the period 2010–2023 were extracted from the Geological Survey of Denmark and Greenland (2023).

2.2. Floating chambers for gas flux measurements

To obtain continuous measurements of CH_4 and CO_2 fluxes, we used the floating chamber design described by Bastviken et al. (2020), applied by Sieczko et al. (2020), and used in an automated version by Martinsen et al. (2018) Fig. S1). This design is a do-it-yourself and cost-efficient approach for measuring CH_4 (NGM2611-E13, Figaro, USA) and CO_2 (CO2 K33 ELG, SenseAir, Sweden) concentrations and auxiliary variables (humidity and temperature) at high resolution (every 2 s for CH_4, humidity, and temperature and 20 s for CO_2) in the floating chamber's headspace. The sensors are connected to an Arduino (Arduino Uno Rev3, USA) that controls the sensors and records the signals. The floating chambers were made from PVC buckets (volume = 0.0135 m^3; surface area = 0.06 m^2) with a polystyrene floating collar. Each chamber was equipped with an air pump (DC radial blower, RS pro, flow capacity = 1.13 l s^{-1}), replacing the floating chamber air headspace at regular intervals to enable automatic and continuous measurements of CH_4 and CO_2 fluxes as described in (Martinsen et al., 2018). Preparatory experiments confirmed that cycles with 20 min of air exchange (air pump on) followed by a 40-minute measurement period (air pump off) were appropriate. An air inlet and an outlet

with a 1.5 m long PVC hose (diameter = 16 mm) were placed on each side of the bucket. The inlet hose was connected to the pump, while the outlet hose serves as a passive relief valve to prevent pressure build-up. The size, length, and type of the hose used were chosen to maximize exchange capacity of the chamber air headspace (100 times during a 20-minute pump cycle), while minimizing air pump power consumption and diffusive gas exchange between the chamber's air headspace and the atmosphere during measurements. Each floating chamber was powered by an 18 Ah 4S $LiFePO_4$ battery, placed in a polystyrene box next to the chamber. Floating chambers were tied to a sunk float which was held in place by an anchor, allowing the chamber to drift approximately 1 m to each side without disturbing the anchor and creating ebullition.

Calibration of the CH_4 sensors was done following the procedure outlined in Bastviken et al. (2020). The CO_2 sensors were pre-calibrated by the manufacturer. Methane sensors were calibrated in atmospheric air with injections of methane, measuring at a minimum of nine different CH_4 concentrations spanning 0–120 ppm. Furthermore, due to the measurement principle of metal oxide gas sensors, the sensor resistance increases with decreasing humidity. Thus, calibration was performed at three or more humidity levels to determine background resistance for each sensor at different CH_4 values (see Bastviken et al. (2020) for more details). A Gasmet DX4030 FTIR Gas Analyzer (Version E1.22, Finland) and a Los Gatos Microportable Greenhouse Gas Analyzer (GLA131-GPC ABB, Switzerland) were used to measure the CH_4 concentration within the calibration chamber. Each sensor was calibrated before and after deployment; we did not find any drift during the five-day measurement campaign.

2.3. Field measurements

In Lake Lyng, a total of 80 temporary stations (1–80) were distributed evenly across transects covering the entire lake (Fig. 1). Floating chambers measured CO_2 and CH_4 fluxes at each station for 16–21 h before being moved to the next station. For example, chamber number 1 measured at stations 1–4 over the five-day sampling campaign, chamber 2 measured at stations 5–8, and so on. Additionally, fluxes were measured at the five permanent stations throughout the five days, which were chosen to represent differences in depth and sediment conditions. Both temporary and permanent stations were used to ensure high spatial coverage on each day, as well as being able to obtain high number of replicate flux measurements that could correct for any possible differences between days. A total of 24 flux chambers were deployed throughout the sampling period, except for the first day, when only 23 were deployed. All chambers were placed within approx. 0.5 m of the station using the GPS of the sonar (Lowrance HDS-12 Gen3 GPS;). Prior to deployment, all CO_2 and CH_4 sensors were switched on for 1 h or longer to enable the CH_4 sensor to warm up. We then confirmed that measurements were correct and calibrated the sensors with reference to the atmospheric concentration.

2.4. Flux calculations

CH_4 fluxes ($F_{CH4\text{-}total}$) were separated into ebullitive ($F_{CH4\text{-}ebul}$) and diffusive fluxes ($F_{CH4\text{-}diff}$). Only the diffusive flux of CO_2 (F_{CO2}) was considered, as no ebullitive CO_2 flux occurred due to the high solubility of CO_2 in water. A 10-point moving average was repeated five times, as proposed by Kajiura and Tokida (2021), to minimize noise from the low-bit analog-to-digital converter of the Arduino. Fluxes (μmol m^{-2} h^{-1}) were calculated using the equation:

$$F = \frac{dC}{dt}\frac{P_{amb}V}{R_{gas}TA}, \quad (1)$$

where the first term (dC dt^{-1}) is the rate of change (ppm h^{-1}) of either CH_4 or CO_2 in the chamber's headspace, P_{amb} is the ambient pressure (Pa), V is the chamber's headspace volume (m^3), R_{gas} is the ideal gas constant (m^3 Pa K^{-1} mol^{-1}), T is the ambient temperature (K), and A is the surface area of the flux chamber in contact with the water surface (m^2). A positive flux denotes transport from water (source) to the atmosphere and a negative flux denotes transport from the atmosphere to the water (sink).

From the high-frequency time series collected for each flux measurement, we separated the CH_4 chamber headspace signal into $F_{CH4\text{-}diff}$ and $F_{CH4\text{-}ebul}$ by identifying ebullitive events that were characterized by a fast increase in CH_4 (Fig. S2). We used a 5-point running variance filter to identify any sudden increase in the time series caused by an ebullitive event and applied a threshold value (0.1–0.5) to distinguish ebullitive events from the running variance. We determined a threshold value in an iterative process for each station based on a visual inspection of the CH_4 concentration and the running variance time series. For each ebullitive event, we determined the minimum and maximum CH_4 concentrations including all CH_4 concentrations 1 min before and after the ebullitive event, to ensure the inclusion of the entire CH_4 concentration change. Events recorded as ebullitive but with a negative or low (< 2 ppm) change in concentration were removed, since these were most likely false detections of ebullitive events, and very low concentration changes might be due to diffusion.

Prior to the calculation of $F_{CH4\text{-}diff}$, we discarded the first 200 measurements (6.5 min deadband) after replacement of the chamber headspace air to avoid any artifacts such as pressure changes due to deployment, and used up to 400 measuring points (13 min) to calculate a slope (dC dt^{-1} in Eq. (1)) using a linear regression model. The slopes of ebullitive events identified in this period were determined from the measurements leading up to this event. $F_{CH4\text{-}diff}$ was calculated based on at least 50 observations.

F_{CO2} was calculated from chamber headspace CO_2 measurements. Similarly, for $F_{CH4\text{-}diff}$, the slope of concentration over time was determined using a linear regression model. For both F_{CO2} and $F_{CH4\text{-}diff}$, only regression models with $R^2 > 0.5$ were used for further analysis. The extensive sampling campaign in Lake Lyng resulted in 1475 CH_4 flux measurements for 87 'station days'. On average, 12 $F_{CH4\text{-}diff}$ and 14 $F_{CH4\text{-}ebul}$ measurements (minimum of 5) were available for each station. The CO_2 sensor malfunctioned over time in many of the floating chambers, most likely due to moisture accumulation in the sensing region. A total of 748 F_{CO2} measurements were available for 46 'station days' distributed randomly across the lake.

2.5. Statistical analysis

We used linear regression models to investigate drivers of $F_{CH4\text{-}diff}$, $F_{CH4\text{-}ebul}$, and F_{CO2} based on daily station averages. Prior to modeling, we assessed the correlation between the predictor variables using Spearman rank correlation. Variables with a Spearman ρ between −0.39 and 0.39 were kept, indicating no relationship between the two variables, while only one variable was kept if this threshold was exceeded based on correlation with the response variable. We fitted models with $F_{CH4\text{-}diff}$, $F_{CH4\text{-}ebul}$, and F_{CO2} as the response variables. For $F_{CH4\text{-}diff}$, we used average oxygen concentration, sediment hardness, and aquatic plant coverage as the predictor variables. For $F_{CH4\text{-}ebul}$, we used water depth, sediment hardness, aquatic plant coverage, and wind fetch (the unobstructed travel length of wind across the water surface from a given direction) as the predictor variables. For F_{CO2}, we used sediment hardness, wind gust, latitude, and longitude. For all models, we performed model selection using a stepwise backward elimination approach, in which predictor variables were removed until all remaining variables were either significant ($p < 0.05$) or showed a tendency ($p < 0.1$). A full list of all predictor variables can be found in the supplement (Table S1).

We performed a simple simulation to determine the number of daily flux measurements needed to measure representative lake levels for $F_{CH4\text{-}diff}$, $F_{CH4\text{-}ebul}$, and F_{CO2}. We randomly selected a number of daily fluxes 1000 times and compared these to the lake's actual average daily flux. The number of daily fluxes varied from 1 to 87 (87 being the maximum number of daily fluxes). For F_{CO2} only 46 daily fluxes were available. An arbitrary high precision boundary of the average daily flux of ±20 % was used, similar to Wik et al. (2016). When 95 % of the random draws reached this threshold, the number of daily fluxes was assumed to be sufficient.

We visualized whole lake fluxes by interpolating station measurements for the three fluxes and average oxygen concentration above the sediment. This was done using inverse distance weighted interpolation with an inverse distance power set to 1.

3. Results

3.1. Environmental conditions

In autumn 2021, we carried out an intensive measurement campaign in Lake Lyng, quantifying CO_2 and CH_4 flux and a wide range of candidate predictor variables expected to be important for producing and exchanging these greenhouse gases. Wind speeds were generally low (mean 0.7 m s^{-1}), with higher values during daytime (mean 0.9 m s^{-1}, range 0–3.1 m s^{-1}) than nighttime (mean 0.6 m s^{-1}, range 0–3.3; Fig. 2) and daytime gust wind speeds approximately 4-times higher than nighttime gusts. Daily incoming irradiance as PAR (photosynthetically active radiation, 400–700 nm) averaged 11.4 mol m^{-2} d^{-1}, while air temperature was quite variable (7.8 to 18.6 °C) and atmospheric pressure very constant (1009 to 1022 hPa: Fig. 2). Water temperature profiles revealed a thermocline at approximately 5.5-m depth with epilimnion temperatures of 14–16 °C and hypolimnion temperatures of 10.5–11.5 °C (Fig. 2). Daily mean oxygen concentrations at 0.5 m above the sediment ranged between 0.02 and 3.8 mg O_2 l^{-1} below 5 m water depth (Fig. S3) and in the northern part (1.4–3.8 mg O_2 l^{-1}), whereas levels were between 8 and 10 mg O_2 l^{-1} above 5 m water depth.

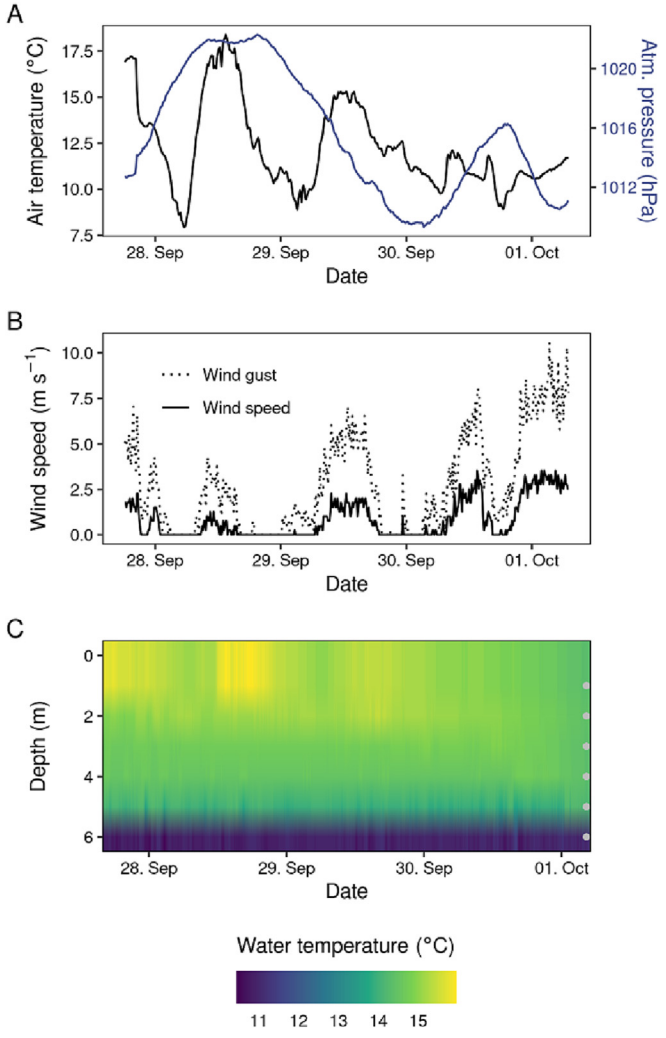

Fig. 2. Environmental conditions during the five-day measuring period. A) Air temperature (black) and atmospheric pressure (blue, secondary y-axis). B) Wind speed (solid line) and gust wind speed (dotted line). C) Isopleth of water temperature from the deepest part of the lake. Grey dots denote the depth of water temperature sensors. (For interpretation of the references to colour in this figure legend, the reader is referred to the web version of this article.)

Alkalinity in Lake Lyng was 0.9 meq. l^{-1}, while pH in surface waters at the mid-lake station was 7.3 in the early mornings and 7.7 in the evenings, with a mean of 7.5 (Fig. S4). Depth profiles of pH were measured at the five permanent stations on one occasion and showed higher values (7.6) in surface waters than in bottom waters (6.7). Dissolved CO_2 concentrations were above the equilibrium concentration with the atmosphere (about 18 μmol CO_2 l^{-1}) both during daytime and nighttime (Fig. S4; mean 52, range 24.8–72.2 μmol CO_2 l^{-1}, Fig. S4). Daytime decrease in CO_2 concentrations correlated with higher wind speed (Fig. S4).

Submerged plants were present at 1–4 m water depth, while deeper and shallower areas had no plants. Shallow areas (< 1 m water depth) were dominated by the reed *Typha angustifolia*, while intermediate water depths (1–4 m) had submerged plants. The average plant coverage at the stations was low (mean 5.8 %), but the southern part of the lake had high coverage at some stations (mean 31 %, range 1–80 %). Submerged plant coverage was low in the western and northern parts of the lake (Fig. S4).

Sediment hardness showed high spatial variability across the lake bottom, particularly at water depths above 5 m (Fig. S5). Sediment hardness was generally lower (i.e., softer sediments) in the deeper parts (> 5 m) and in wind-sheltered, shallow water in the western and northern parts. Areas with steeper slopes showed higher sediment hardness. This was the case for depths of 4–6 m leading to the deepest part of the lake. In contrast, areas with a small slope or a plateau showed lower sediment hardness. This was mainly observed for depths of 2–4 m.

3.1.1. Ebullitive CH_4 fluxes

$F_{CH4\text{-}ebul}$ was highest in the deepest parts and less in the shallower parts of the lake (Fig. 3). $F_{CH4\text{-}ebul}$ showed no diel pattern over the five-day sampling period and no difference between daytime and nighttime values (Fig. 4, diel mean 54.8 μmol CH_4 m^{-2} h^{-1}; paired *t*-test, $t = 0.06$, df = 72, $p = 0.95$). $F_{CH4\text{-}ebul}$ increased towards the end of the campaign, while the probability of ebullition events did not change systematically (Fig. 4). Only a few ebullitive events occurred during the first two days while higher flux rates occurred on days three and four, followed by a further increase on day five (Fig. 4). $F_{CH4\text{-}ebul}$ for the entire lake averaged at 54.8 μmol CH_4 m^{-2} h^{-1}, which was determined by interpolation between sites (Fig. 3).

3.1.2. Diffusive CH_4 fluxes

The spatial variability of $F_{CH4\text{-}diff}$ was generally lower than for $F_{CH4\text{-}ebul}$ (Fig. 3). Average $F_{CH4\text{-}diff}$ showed small diel variations but were significantly higher during daytime compared to nighttime (Fig. 4, daytime mean 19.5 and nighttime mean 15.0 μmol CH_4 m^{-2} h^{-1}; paired *t*-test, $t = 2.9$, df = 69, $p = 0.005$). $F_{CH4\text{-}diff}$ increased towards the end of the campaign but was of low magnitude. $F_{CH4\text{-}diff}$ and $F_{CH4\text{-}ebul}$ were significantly positively related but the proportion of explained variation was very low (linear regression model, $n = 1409$, t-value = 5, $p < 0.001$, $R^2 = 0.02$). $F_{CH4\text{-}diff}$ for the entire lake averaged 13.6 μmol CH_4 m^{-2} h^{-1}, which was determined by interpolation between sites (Fig. 3). Some stations had negative $F_{CH4\text{-}diff}$, but most negative values were low (mean − 18 μmol CH_4 m^{-2} h^{-1}) and close to the detection limit of the setup (Bastviken et al., 2020).

3.2. CO_2 fluxes

F_{CO2} exhibited substantial temporal variability both within and between days which was characterized by few CO_2 influxes and large CO_2 effluxes (mean 919, range − 3941 to 5667 μmol CO_2 m^{-2} h^{-1}; Fig. 4). F_{CO2} tended to be higher during daytime than nighttime, but this difference was not significant (daytime mean 935, nighttime mean 778 μmol CO_2 m^{-2} h^{-1}; paired *t*-test, $t = 0.8$, df = 36, $p = 0.43$). $F_{CO2\text{-}diff}$ for the entire lake averaged at 1127 μmol CO_2 m^{-2} h^{-1}, which was determined by

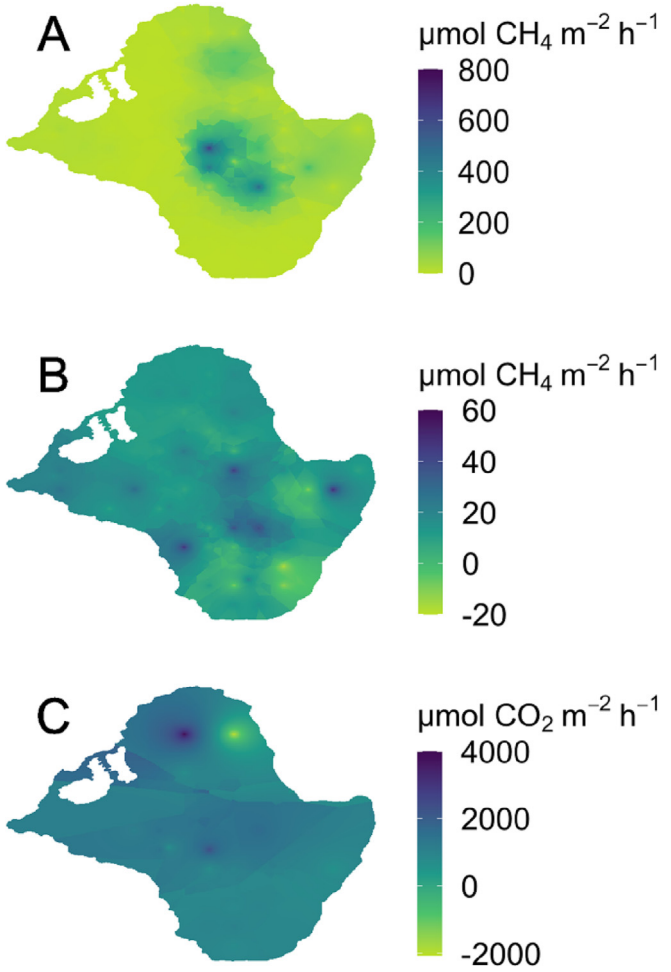

Fig. 3. Interpolated maps of (A) ebullitive methane flux, (B) diffusive methane flux, and (C) diffusive CO_2 flux over five days in Lake Lyng. The magnitude of rates is shown by the colour bars.

interpolation between sites (Fig. 3). There was no systematic spatial pattern in F_{CO2}, though higher fluxes occurred from mid-lake deeper waters. An area above a depression in the lake bottom with hypoxic water (station '20', Fig. 1 + S2) had the highest F_{CO2} and released almost twice the amount as the station with the second-largest flux.

3.3. Drivers of gas fluxes

Two models of methane fluxes were fitted with $F_{CH4\text{-}ebul}$ and $F_{CH4\text{-}diff}$, respectively, as the response variables. The final $F_{CH4\text{-}ebul}$ model contained one significant variable, showing an increase of ebullitive flux from deeper water (65 ± 10, $p < 0.001$, $R^2 = 0.32$, $F = 42$, $df = 86$). The final $F_{CH4\text{-}diff}$ model included plant coverage (-6.1 ± 1.2, $p < 0.001$) and sediment hardness (-2.5 ± 1.1, $p = 0.03$; $R^2 = 0.30$, $F = 19$, $df = 83$), both significantly related to diffusive methane flux. The final F_{CO2} model contained two significant predictor variables: wind gust (0.54 ± 0.14, $p = 0.001$) and longitudinal position (-0.38 ± 0.19, $p < 0.05$; $R^2 = 0.24$, $F = 8.2$, $df = 43$). Wind gust and longitudinal position showed positive and negative relationships, respectively, with CO_2 flux.

Six groundwater wells, located within 2 km from Lake Lyng, contained 0.31–0.62 μmol CH_4 l^{-1} and 659.1–1091 μmol CO_2 l^{-1}. Applying the expected groundwater flow multiplied by the and dissolved gas concentration within Lake Lyng's catchment, we calculate that the lake relative to its surface area receives only 0.43–0.86 nmol CH_4 m^{-2} h^{-1} and 0.92–1.5 μmol CO_2 m^{-2} h^{-1}.

3.4. Sampling intensity for accurate measurement of whole-lake CH_4 and CO_2 fluxes

Simulation of the number of daily fluxes measured across the lake surface, to determine the average whole-lake daily $F_{CH4\text{-}ebul}$, $F_{CH4\text{-}diff}$, and F_{CO2} with high certainty, revealed large differences (Fig. 5). Especially $F_{CH4\text{-}ebul}$ required a high number of daily flux measurements (> 70) to be within 20 % of the average daily flux. For $F_{CH4\text{-}diff}$, approx. 39 daily flux measurements were needed to be within the 20 % range of the average daily flux, and for F_{CO2}, approx. 27 daily flux measurements were required. Too few measurements (≤ 10) of daily ebullitive fluxes could lead to an overestimation of average daily fluxes by a factor of 3–12 or, alternatively, an underestimation, resulting in values as low as 0–4 % of the average daily ebullitive fluxes.

4. Discussion

CH_4 and CO_2 fluxes are expected to display different spatiotemporal patterns depending on the specific gas and the type of gas flux, either diffusion from the water surface or ebullition due to bubble release from sediments. Logically, the observed patterns should reflect differences in biological processes and physical regulations underlying diffusive fluxes and ebullition. Methane mainly is produced by anaerobic respiration in the sediments and oxidized by anaerobic and aerobic processes in sediments and water (Bastviken, 2009; Fenchel et al., 2012), whereas CO_2 is formed by aerobic and anaerobic respiration in sediments and water and consumed by photosynthesis in illuminated sediments and water layers (Fenchel et al., 2012). Moreover, CH_4 and CO_2 effluxes may derive from an external input of soil water with high concentrations of these gases (McDonald et al., 2013). Lake Lyng receives water from surface runoff and groundwater input, the latter containing elevated CH_4 and CO_2 concentrations. However, due to the small effective catchment area and low concentrations, the groundwater inputs CH_4 or CO_2 were negligible compared to the in-lake carbon conversion processes and gas effluxes from the lake.

4.1. Ebullitive CH_4 fluxes

CH_4 release by ebullition is a highly stochastic process, occurring when production rates of CH_4 exceed losses by anaerobic and aerobic CH_4 oxidation and diffusion from the sediment surface (Bastviken, 2009). Bubbles rich in CH_4 may form, grow, and obtain a buoyancy that overcomes the combined atmospheric and hydrostatic pressure and the physical resistance to release from the sediment matrix (Boudreau, 2012; Katsman et al., 2013). An initial bubble release, with or without physical disturbance by water flow above the sediment, may weaken sediment resistance and give rise to a stream of bubbles (Delwiche et al., 2015). Subsequently, it may take a while before the sediment site has produced sufficient CH_4 to release bubbles again. The temporal variability of bubble release from one site compared to another may reflect temporal variations in the interactions of physical and biological processes at the sites (Bastviken, 2009; Bastviken et al., 2004).

We recorded 476 ebullitive events in 1.9 million measurements during five days with 24 floating chambers. The recorded events are probably a small underestimation of bubble release because it is difficult to distinguish between bubbles that enter a floating chamber within two seconds of each other. Nonetheless, considering the small surface area covered by the floating chambers relative to the lake surface area, the daily mean number of bubbles is 7.9 per m^2 of surface area, but almost 800,000 for the entire 10-ha lake. These values stress that CH_4 ebullition can be intense in eutrophic lakes like Lake Lyng, even outside the warm summer period when ebullition is expected to peak (Langenegger et al., 2019).

While a few permanent stations recorded an above-average number of ebullitive events during the last two days of the study period, this spatiotemporal variation was not apparent when considering all stations together. Previous studies have attributed episodic ebullitive events to a sudden drop

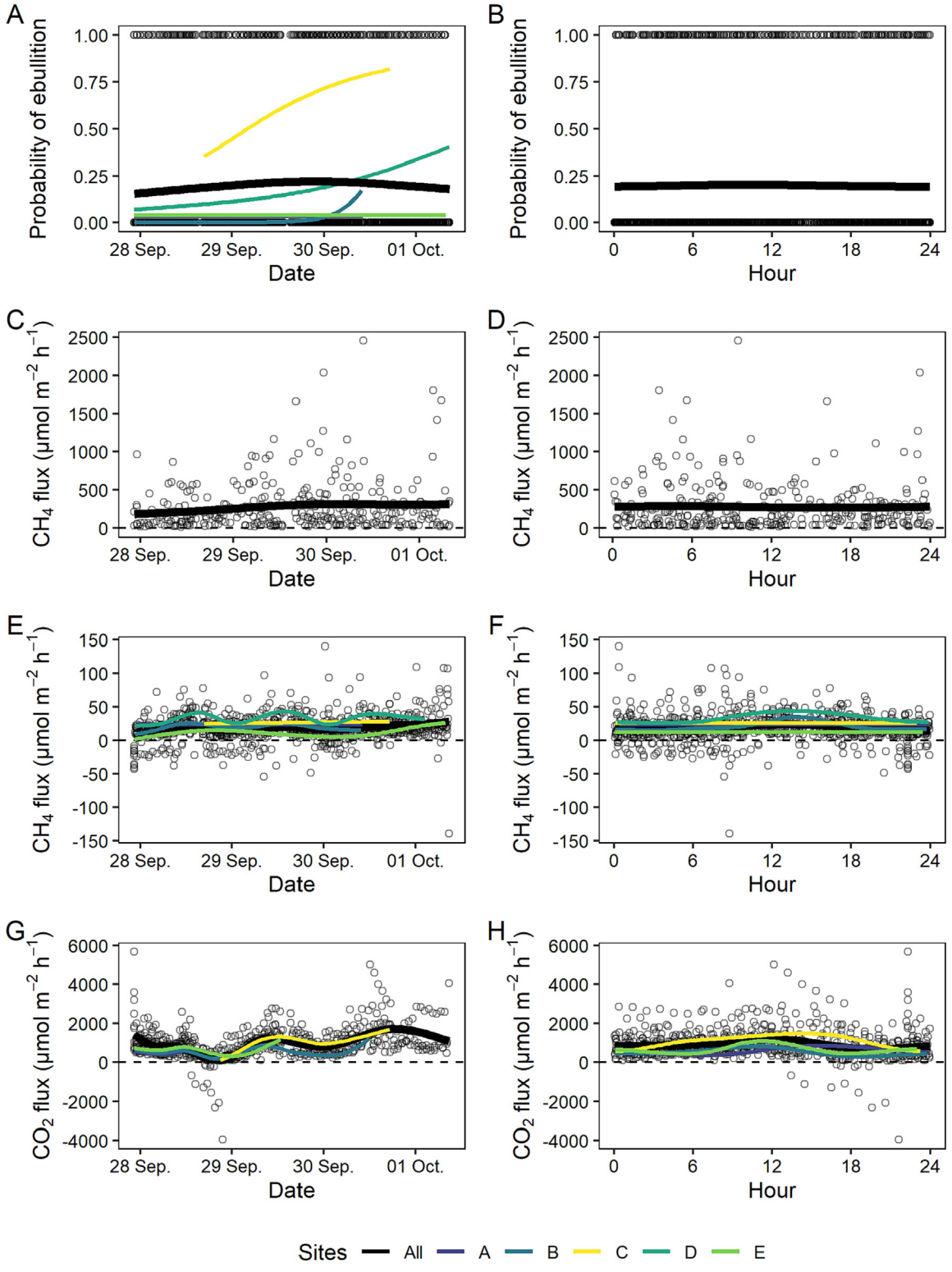

Fig. 4. Temporal variability of fluxes of $F_{CH4\text{-}ebul}$, $F_{CH4\text{-}diff}$, and F_{CO2} both during the entire measuring campaign (A, C, E, G) and throughout the day (B, D, F, H). Grey points are flux measurements, and solid lines are generalized additive models where different distributions are assumed (A-D are Gaussian, *E*-F are Binomial, and G-H are Gamma). The black line indicates all measurements, while the others indicate the permanent stations.

in atmospheric pressure and an increase in wind speed (Joyce and Jewell, 2003; Varadharajan and Hemond, 2012). Although these effects were not specifically tested in our study, we did record a drop in atmospheric pressure on 29 September, the day with the most ebullitive events and highest $F_{CH4\text{-}ebul}$. Although wind speed varied through the measuring period, the frequency of ebullitive events, or the magnitude of fluxes did not correlate with wind speed. In fact, the highest wind speed was recorded on 1 October, yet $F_{CH4\text{-}ebul}$ decreased. Furthermore, wind speeds showed large diel variations but did not correlate with the frequency of ebullitive events or the magnitude of $F_{CH4\text{-}ebul}$. However, we acknowledge that the study period was short, and the magnitude and variability of wind speed on the small, sheltered Lake Lyng was probably too low to generate substantial changes

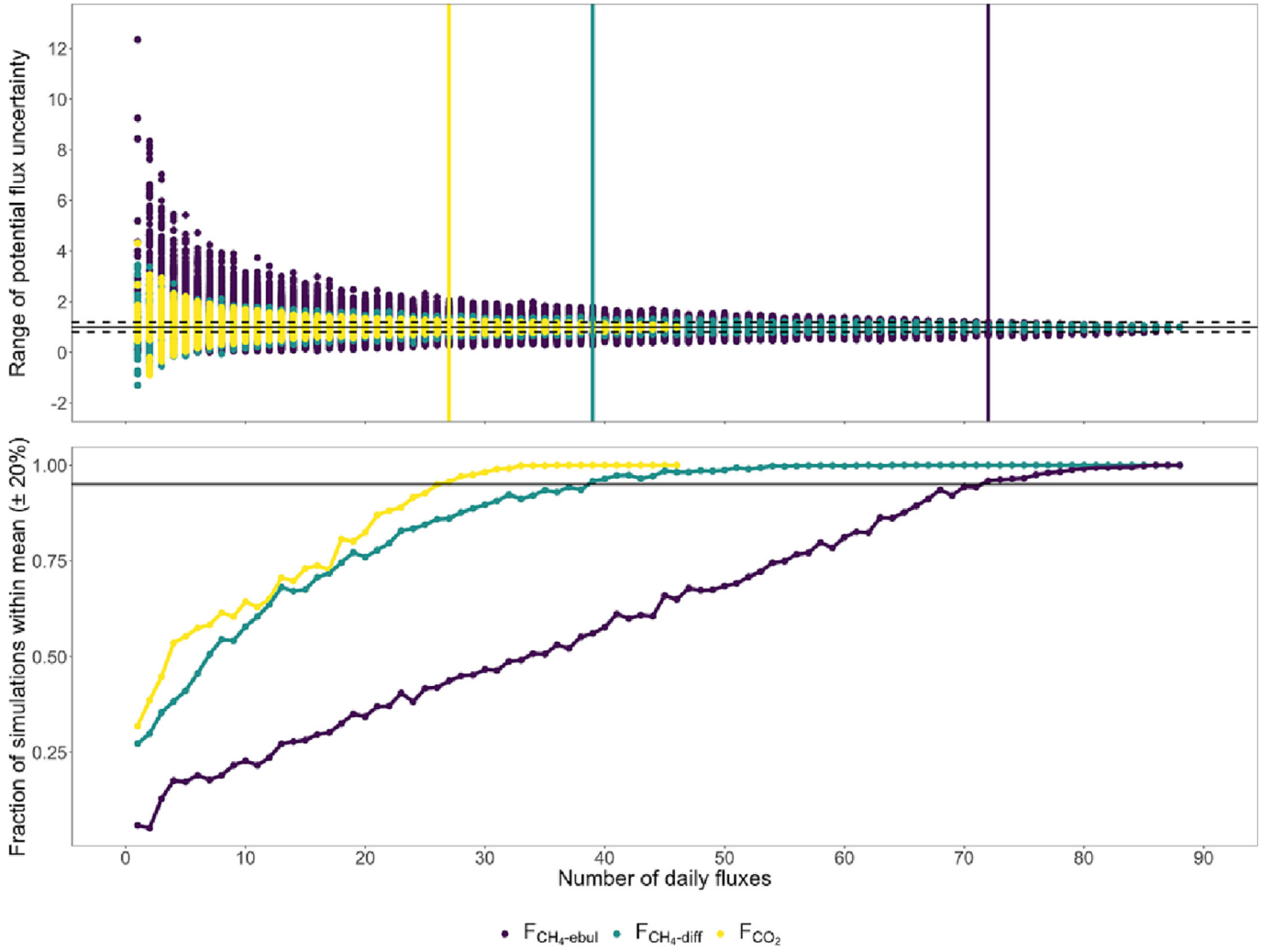

Fig. 5. Simulation of the number of daily fluxes required to attain mean values within + − 20 % of the overall lake average of ebullitive (purple) and diffusive (green)) CH_4 flux and diffusive CO_2 flux (yellow) over five days in Lake Lyng. (For interpretation of the references to colour in this figure legend, the reader is referred to the web version of this article.)

of wind-induced shear on sediments and, thereby, potentially influence CH_4 ebullition.

Methane ebullition in Lake Lyng increased towards areas deeper than 3 m, while areas shallower than 2 m had little or no release. Ebullition has previously been found to change with water depth, but some studies report a decrease with depth (Bastviken, 2009; Bastviken et al., 2004), while others report an increase (Schilder et al., 2016). We found a significantly higher $F_{CH4\text{-ebul}}$ in deep water, which also had significantly lower oxygen concentrations caused by stratification and only slightly lower temperature above the sediments. Stratification of lake water promotes the presence and most likely a greater abundance of active methanogenic bacteria (Lyautey et al., 2021), while also inhibiting the oxidation of CH_4 due to anoxic conditions in the deeper water. Sediments in the deeper water of Lake Lyng were softer and thereby possibly richer in organic matter, which is likely promoted by sediment focusing as a consequence of the lake's bathymetry (Håkanson and Jansson, 1983). The input of labile organic matter from primary production in the surface waters to deep, anoxic hypolimnion sediments has been shown in other studies to fuel methane formation (Grasset et al., 2018). However, we found no significant relationship between $F_{CH4\text{-ebul}}$ and sediment hardness, indicating that the methane formation caused by an input of organic matter does not emit as bubbles, but rather by diffusion. Although no significant relationship was present, we do believe that variation of sediment organic matter content influences the magnitude of CH_4 formation and emission. Some authors have suggested that greater hydrostatic pressure in deeper water prevents bubbles from being released from the sediment (Bastviken et al., 2004). However, an increase of water depth from 2 m to 7 m only increases the combined air and hydrostatic pressure from 1.2 to 1.7 atm. This small difference cannot explain the 40 % higher net release rate of CH_4 from water depths of 7 m relative to 2 m in Lake Lyng. Furthermore, the amount of CH_4 in the bubbles that gets dissolved during the passage from 7 m depth to the surface is expected to be small: Estimates from a similar type of lake show that only 14 % of the CH_4 content was dissolved from a 6 mm diameter bubble traveling 6 m, from the sediment surface at 10 m depth to a CH_4 trap positioned 4 m below the water surface (Langenegger et al., 2019). As long as the depth range is modest (e.g., 0–20 m), CH_4 ebullition should not markedly decrease with water depth as bubbles may still reach the required size and positive buoyancy to being released. When bubble release from sediments at modest water depth does not occur, it is more likely due to a combination of lower temperature, low sedimentation rates, and predominance of old, recalcitrant organic matter in the sediment lowering CH_4 production rates (Grasset et al., 2018). Accordingly, we propose that patterns of ebullition in shallow lakes should change with lake trophy and bathymetry influencing the settling rate and quality of organic particles as well as temperatures and oxygen concentrations in bottom waters influencing CH_4 production.

4.2. Diffusive CH_4 fluxes

As expected, the diffusive CH_4 flux in Lake Lyng showed higher diel variation than the ebullitive CH_4 flux. Diffusive fluxes of CH_4 were higher during daytime than nighttime and were positively correlated with higher wind speeds, which increase the gas transfer velocity (Heiskanen et al., 2014). Other studies have reported different diel patterns; e.g., Zhang et al. (2019) found the highest diffusive fluxes of CH_4 in the spring during nighttime, while Podgrajsek et al. (2014) observed the highest diffusive CH_4 fluxes after sunrise and in the evening, but found no correlation to wind speed.

The relationship between sediment hardness and $F_{CH4\text{-}diff}$ suggested that sediment characteristics influence CH_4 formation in Lake Lyng, with softer sediments causing higher methane formation compared to harder sediments. Lakes with sediments rich in organic matter have previously been shown to have high CH_4 flux compared with lakes of lower organic content (Bastviken et al., 2004). However, variations within lakes have not been studied in detail. We found no significant relationship between sediment density and sediment organic matter, likely due to difficulties related to locating the exact sampling site of sediment cores. Moreover, when CH_4 is released from the sediment it disperses both vertically and horizontally through the water column, $F_{CH4\text{-}diff}$ observed using floating chambers is proportional to the CH_4 concentration gradient and transfer velocity and therefore only weakly related to sediment characteristics below the floating chamber. Finally, the lability of the sediment organic matter likely has a stronger effect on CH_4 formation than the bulk content of organic matter per se (Grasset et al., 2018).

The effect of vegetation on CH_4 fluxes has focused mostly on emergent plants working as methane release vents (Desrosiers et al., 2022). Only a few studies have looked at the role of submerged aquatic plants in CH_4 fluxes. Aquatic plants may increase the input of organic litter to the lake floor, which in turn could be degraded and form CH_4 (Mille-Lindblom and Tranvik, 2003), but in contrast rooted aquatic plants may reduce CH_4 concentrations in sediments due to root oxygen release into the sediment (Sand-Jensen et al., 1982). Furthermore, root surfaces and above-ground shoots create habitats for CH_4 oxidizing methanotrophs (Mille-Lindblom and Tranvik, 2003; Sorrell et al., 2002). In fact, plant coverage negatively correlated with $F_{CH4\text{-}diff}$, and a CH_4 influx from the atmosphere to water was observed in areas with the highest plant coverage, which may be due to methanotrophs attached to leaf surfaces.

4.3. Diffusive CO_2 fluxes

CO_2 flux from lakes is often lower during daytime compared to nighttime due to photosynthesis (Kling et al., 1992). Calculations of surface water CO_2 concentration from pH and alkalinity sampled at the center of Lake Lyng showed permanent supersaturation of CO_2 relative to the atmosphere throughout the entire period, with modest daytime reduction of CO_2 concentrations (Fig. S4). Decreasing CO_2 concentrations occurred simultaneously with the occurrence of increasing wind, which further points to the importance of wind speed and its influence on the gas transfer velocity as the main predictor of CO_2 fluxes and thereby surface water CO_2 concentration in Lake Lyng. We a priori expected a diel effect of plant coverage on CO_2 fluxes due to higher photosynthesis and CO_2 utilization during daytime, whereas higher CO_2 fluxes were expected during nighttime due to ongoing respiration and possibly higher rates in areas with submerged plants. Furthermore, litter from the aquatic plants could supply organic matter to decomposing bacteria, thereby increasing the nighttime CO_2 flux. However, no diel, nor plant, relationship was found in our models. We speculate that the lack of significant impact in our model may be due to low plant coverage or low irradiance during the measuring period in Lake Lyng. Conversely, diffusive CO_2 efflux in Lake Lyng was higher during daytime than nighttime which may be due to the higher daytime wind speed and resulting higher gas transfer velocity.

4.4. Influence of spatiotemporal variability on whole-lake flux estimates

We applied automated floating chambers to collect hourly measurements of diffusive and ebullitive fluxes of CO_2 and CH_4. Changes in CH_4 concentrations were measured at high time resolution in the chambers' headspace air, enabling us to separate between diffusive and ebullitive fluxes by identifying individual bubble events when they were separated by more than just a few seconds. In comparison, traditional deployment of floating chambers followed by withdrawal of chamber headspace air for analysis cannot distinguish diffusive from ebullitive fluxes, and short-term measurements are cumbersome. Bubble traps such as inverted funnels (Keller and Stallard, 1994) cannot assess the size and content of individual bubbles, and the temporal resolution is modest, though relatively short, repeated incubation periods are possible. These shortcomings are probably the main reasons why studies of gas fluxes with a high spatiotemporal resolution are that few.

One disadvantage of our setup was the sub-optimal resolution of the analog-to-digital converter, making it hard to distinguish between small changes in CH_4 concentrations. Furthermore, separation of ebullitive and diffusive fluxes was sometimes difficult, and there may have been cases where ebullitive events were missed, though they represent a small and insignificant fraction of the total. Future studies should attempt to improve methods for identifying short-term ebullitive events (e.g., Delwiche et al. (2015)).

In situ measurements of CH_4 and CO_2 fluxes have long been time-consuming, as numerous measurements are needed due to the large heterogeneity of fluxes, particularly for ebullition. Compromises are needed when selecting a number of sites and frequency of measurements. Wik et al. (2016) estimated the minimum number of measurement sites needed to determine the average whole-lake flux. Our study is, to our knowledge, the first with the sufficient spatial resolution of CH_4 and CO_2 fluxes from a whole lake, ensuring high-accuracy determination of mean whole-lake fluxes for a selected period.

Measurements showed extensive spatiotemporal variability of all fluxes but particularly high variability of CH_4 ebullition. Thus, the 72 daily fluxes for 10-ha Lake Lyng to attain a reliable mean whole-lake value of CH_4 ebullition was close to the 88 daily flux measurements conducted. An additional simulation was made considering the water depth (not shown), in which the lake was divided into two depth intervals (0–3 m and > 3 m) to investigate if this would reduce the number of daily flux measurements needed to attain a better mean estimate of the entire lake fluxes. However, this procedure did not change previous simulations suggesting no effect of depth. Nonetheless, water depth did show significant effect on the ebullitive flux, while the simulation with and without depth included showed no difference. Use of more than two depth intervals was not tested. The temporal and spatial resolution is much lower in contemporary studies, stressing that finer temporal and spatial resolution is required in the future by the traditional use of floating chambers to attain reliable whole-lake mean values. Lakes with complex bathymetry will increase the required spatial coverage even further to obtain reliable whole-lake estimates compared with the small Lake Lyng. Thus, we see three future directions for quantification of whole-lake CH_4 fluxes: 1) use a high number of floating chambers with a high temporal resolution; 2) apply an eddy covariance method to cover the entire lake (Aubinet et al., 2012); and 3) apply a mass balance approach directed at quantifying CH_4 production and release from the sediment and loss in the water column (e.g., Langenegger et al. (2019)). Our approach (1) has the potential to determine underlying drivers of spatial and temporal variability of CH_4 and CO_2 fluxes.

5. Conclusions

During five days intensive measurements in Lake Lyng, we estimated 800,000 bubble events, which were the primary source to CH_4 flux from the lake (mean 68.4 μmol CH_4 m^{-2} h^{-1}). Concurrently, the mean diffusive CO_2 efflux was 1127 μmol CO_2 m^{-2} h^{-1}. Our results are in the lower end of values for other small lakes (Rosentreter et al., 2021), which is likely due to

our autumn sampling period. The automatic floating chambers collected numerous measurements of CH_4 and CO_2 fluxes revealing spatiotemporal patterns and offering accurate whole-lake estimates of CH_4 and CO_2 emissions. The low cost of the automated floating chambers also solves the earlier problem of GHG measurements being very expensive. We identified several factors having a significant effect on CH_4 and CO_2 fluxes, although a large proportion of the variance was still unaccounted for in the statistical models. $F_{CH4\text{-}ebul}$ was mainly influenced by water depth, $F_{CH4\text{-}diff}$ by plant coverage and sediment hardness, and F_{CO2} by wind gust and position during the five-days period. Despite sediment hardness only showed a significant correlation with $F_{CH4\text{-}diff}$, we suggest that sediment organic matter and its lability influence the formation rate of CH_4 and CO_2 (Grasset et al., 2018; McDonald et al., 2013). The low explanatory power, particularly regarding ebullitive CH_4 fluxes, suggests that the underlying mechanisms are still not well understood or, alternatively, that they are so complex, intricately regulated, and stochastic that accurate evaluation of drivers of fluxes may be difficult to obtain. In eutrophic, shallow Lake Lyng, CH_4 ebullition is responsible for the main CH_4 loss and future measurements during summer, including better sediment analyses, may improve analysis of drivers.

CRediT author contribution statement

All authors contributed to the conceptualization of the project, with Jonas Stage Sø (JSS), Theis Kragh (TK) and Kaj Sand-Jensen (KSJ) developing the idea of this project. Development of equipment was done by JSS and TK. Formal analysis was performed by JSS and Kenneth Thorø Martinsen (KTM), while investigation was done by JSS, TK, EP and JEK. Visualization was done by JSS and KTM. Writing the original draft was done by JSS, while reviewing and editing was done by all authors. Funding acquisition was done by TK, KSJ and Kasper Reitzel (KR).

Data availability

Data will be made available on request.

Declaration of competing interest

The authors declare that they have no known competing financial interests or personal relationships that could have appeared to influence the work reported in this paper.

Acknowledgments

The work is part of the project “Supporting climate and biodiversity by rewetting low-lying areas” from the Independent Research Fund Denmark (0217-00112B) to KSJ. We thank Aage V. Jensen's foundation for grants supporting the PhD research of JSS. We are thankful for the CH_4 sensors funded by the COWI foundation (A-155.03) and the Carlsberg grant for funding the Ultraportable Greenhouse Gas Analyzer (CF21-0166). We thank David Bastviken for discussions of our approach and results and David Stuligross for proof-reading the manuscript.

Appendix A. Supplementary data

Supplementary data to this article can be found online at https://doi.org/10.1016/j.scitotenv.2023.162895.

References

Andersen, M.R., Sand-Jensen, K., Iestyn Woolway, R., Jones, I.D., 2017. Profound daily vertical stratification and mixing in a small, shallow, wind-exposed lake with submerged macrophytes. Aquat. Sci. 79 (2), 395–406. https://doi.org/10.1007/s00027-016-0505-0.

Andrade, C., Viveiros, F., Cruz, J.V., Coutinho, R., Silva, C., 2016. Estimation of the CO2 flux from Furnas volcanic Lake (São Miguel, Azores). J. Volcanol. Geotherm. Res. 315, 51–64. https://doi.org/10.1016/j.jvolgeores.2016.02.005.

Aubinet, M., Vesala, T., Papale, D., 2012. Eddy Covariance: A Practical Guide to Measurement And Data Analysis. Springer Science & Business Media.

Bastviken, D., 2009. Methane. In: Likens, G.E. (Ed.), Encyclopedia of Inland Waters. Academic Press, Oxford, pp. 783–805.

Bastviken, D., Cole, J., Pace, M., Tranvik, L., 2004. Methane emissions from lakes: dependence of lake characteristics, two regional assessments, and a global estimate. Glob. Biogeochem. Cycles 18 (4). https://doi.org/10.1029/2004gb002238.

Bastviken, D., Nygren, J., Schenk, J., Parellada Massana, R., Duc, N.T., 2020. Technical note: facilitating the use of low-cost methane (CH4) sensors in flux chambers – calibration, data processing, and an open-source make-it-yourself logger. Biogeosciences 17 (13), 3659–3667. https://doi.org/10.5194/bg-17-3659-2020.

Boehrer, B., Schultze, M., 2008. Stratification of lakes. Rev. Geophys. 46 (2).

Boudreau, B.P., 2012. The physics of bubbles in surficial, soft, cohesive sediments. Mar. Pet. Geol. 38 (1), 1–18.

Bundgaard, N.J., Andersen, O.J., Kramer, J., Kjærgaard, J., Jensen, C., Søsted, A., Hansen, A.S., Jørgensen, H., Buhl, E., Granat, H., Trier, L., 2002. . in DanishIn: Trier, L. (Ed.), Silkeborg Statsskovdistrikt - Proposals for the Operation 2000 – 2014. The Danish Environmental Ministry, Board of Forest and Nature.

Delwiche, K., Senft-Grupp, S., Hemond, H., 2015. A novel optical sensor designed to measure methane bubble sizes in situ. Limnol. Oceanogr. Methods 13 (12), 712–721.

Desrosiers, K., DelSontro, T., del Giorgio, P.A., 2022. Disproportionate contribution of vegetated habitats to the CH4 and CO2 budgets of a boreal lake. Ecosystems https://doi.org/10.1007/s10021-021-00730-9.

Enick, R.M., Klara, S.M., 1990. CO2 solubility in water and brine under reservoir conditions. Chem. Eng. Commun. 90 (1), 23–33. https://doi.org/10.1080/00986449008940574.

European Environment Agency, 2019. Trends in atmospheric concentrations of CO2 (ppm), CH4 (ppb) and N2O (ppb), between 1800 and 2017. Retrieved from https://www.eea.europa.eu/data-and-maps/daviz/atmospheric-concentration-of-carbon-dioxide-5#tab-chart_5_filters=%7B%22rowFilters%22%3A%7B%7D%3B%22columnFilters%22%3A%7B%22pre_config_polutant%22%3A%5B%22CO2%20(ppm)%22%5D%7D%7D.

Fenchel, T., Blackburn, H., King, G.M., Blackburn, T.H., 2012. Bacterial Biogeochemistry: The Ecophysiology of Mineral Cycling. Academic press.

Geological Survey of Denmark and Greenland, 2023. Nationalwell database (Jupiter). Retrieved from https://www.geus.dk/produkter-ydelser-og-faciliteter/data-og-kort/grundvandskort-og-data Accessed on the Jan 10, 2023.

Gran, G., 1952. Determination of the equivalence point in potentiometric titrations.Part II. Analyst 77 (920), 661–671.

Grasset, C., Mendonça, R., Villamor Saucedo, G., Bastviken, D., Roland, F., Sobek, S., 2018. Large but variable methane production in anoxic freshwater sediment upon addition of allochthonous and autochthonous organic matter. Limnol. Oceanogr. 63 (4), 1488–1501.

Håkanson, L., Jansson, M., 1983. Principles of Lake SedimentologyVol. 316. Springer-verlag, Berlin.

Heiskanen, J.J., Mammarella, I., Haapanala, S., Pumpanen, J., Vesala, T., MacIntyre, S., Ojala, A., 2014. Effects of cooling and internal wave motions on gas transfer coefficients in a boreal lake. Tellus B: Chem.Phys.Meteorol. 66 (1), 22827.

Hofmann, A.F., Soetaert, K., Middelburg, J.J., Meysman, F.J.R., 2010. AquaEnv: an aquatic acid-base modelling environment in R. Aquat. Geochem. 16 (4), 507–546. https://doi.org/10.1007/s10498-009-9084-1.

Jessen, H., 2021. The weather in Silkeborg. Retrieved from https://www.silkeborg-vejret.dk/om.php Accessed on December 1 2021.

Joyce, J., Jewell, P.W., 2003. Physical controls on methane ebullition from reservoirs and lakes. Environ.Eng.Geosci. 9 (2), 167–178.

Kajiura, M., Tokida, T., 2021. Quantifying bubbling emission (ebullition) of methane from a rice paddy using high-time-resolution concentration data obtained during a closed-chamber measurement. in DanishJ. Agric. Meteorol. 77 (4). https://doi.org/10.21203/rs.3.rs-396475/v1.

Katsman, R., Ostrovsky, I., Makovsky, Y., 2013. Methane bubble growth in fine-grained muddy aquatic sediment: insight from modeling. Earth Planet. Sci. Lett. 377, 336–346.

Keller, M., Stallard, R.F., 1994. Methane emission by bubbling from Gatun Lake,Panama. J. Geophys. Res. Atmos. 99 (D4), 8307–8319. https://doi.org/10.1029/92jd02170.

Kling, G.W., Kipphut, G.W., Miller, M.C., 1992. The flux of CO2 and CH4 from lakes and rivers in arctic Alaska. Hydrobiologia 240 (1), 23–36. https://doi.org/10.1007/BF00013449.

Kragh, T., Sand-Jensen, K., Petersen, K., Kristensen, E., 2017. Fast phosphorus loss by sediment resuspension in a re-established shallow lake on former agricultural fields. Ecol. Eng. 108, 2–9. https://doi.org/10.1016/j.ecoleng.2017.07.026.

Langenegger, T., Vachon, D., Donis, D., McGinnis, D.F., 2019. What the bubble knows: lake methane dynamics revealed by sediment gas bubble composition. Limnol. Oceanogr. 64 (4), 1526–1544.

Lyautey, E., Billard, E., Tissot, N., Jacquet, S., Domaizon, I., 2021. Seasonal dynamics of abundance, structure, and diversity of methanogens and methanotrophs in lake sediments. Microb. Ecol. 82 (3), 559–571. https://doi.org/10.1007/s00248-021-01689-9.

Martinsen, K.T., Kragh, T., Sand-Jensen, K., 2018. Technical note: a simple and cost-efficient automated floating chamber for continuous measurements of carbon dioxide gas flux on lakes. Biogeosciences 15 (18), 5565–5573. https://doi.org/10.5194/bg-15-5565-2018.

McDonald, C.P., Stets, E.G., Striegl, R.G., Butman, D., 2013. Inorganic carbon loading as a primary driver of dissolved carbon dioxide concentrations in the lakes and reservoirs of the contiguous United States. Glob. Biogeochem. Cycles 27 (2), 285–295.

Mille-Lindblom, C., Tranvik, L.J., 2003. Antagonism between bacteria and fungi on decomposing aquatic plant litter. Microb. Ecol. 45 (2), 173–182. https://doi.org/10.1007/s00248-002-2030-z.

Natchimuthu, S., Panneer Selvam, B., Bastviken, D., 2014. Influence of weather variables on methane and carbon dioxide flux from a shallow pond. Biogeochemistry 119 (1), 403–413.

Podgrajsek, E., Sahlée, E., Rutgersson, A., 2014. Diurnal cycle of lake methane flux. J. Geophys.Res.Biogeosci. 119 (3), 236–248.

Rosentreter, J.A., Borges, A.V., Deemer, B.R., Holgerson, M.A., Liu, S., Song, C., Melack, J., Raymond, P.A., Duarte, C.M., Allen, G.H., Olefeldt, D., Poulter, B., Battin, T.I., Eyre, B.D., 2021. Half of global methane emissions come from highly variable aquatic ecosystem sources. Nat. Geosci. 14 (4), 225–230. https://doi.org/10.1038/s41561-021-00715-2.

Sand-Jensen, K., Prahl, C., Stokholm, H., 1982. Oxygen release from roots of submerged aquatic macrophytes. Oikos 349–354.

Sand-Jensen, K., Friberg, N., Murphy, J., 2006. Running Waters Historical Development And Restoration of Lowland Danish Streams. National Environmental Research Institute, Copenhagen.

Sand-Jensen, K., Martinsen, K.T., Jakobsen, A.L., Sø, J.S., Madsen-Østerbye, M., Kjær, J.E., Kristensen, E., Kragh, T., 2021. Large pools and fluxes of carbon, calcium and phosphorus in dense charophyte stands in ponds. Sci. Total Environ. 765, 142792.

Schilder, J., Bastviken, D., van Hardenbroek, M., Kankaala, P., Rinta, P., Stötter, T., Heiri, O., 2013. Spatial heterogeneity and lake morphology affect diffusive greenhouse gas emission estimates of lakes. Geophys. Res. Lett. 40 (21), 5752–5756.

Schilder, J., Bastviken, D., Van Hardenbroek, M., Heiri, O., 2016. Spatiotemporal patterns in methane flux and gas transfer velocity at low wind speeds: implications for upscaling studies on small lakes. J.Geophys.Res.Biogeosci. 121 (6), 1456–1467.

Sieczko, A.K., Duc, N.T., Schenk, J., Pajala, G., Rudberg, D., Sawakuchi, H.O., Bastviken, D., 2020. Diel variability of methane emissions from lakes. Proc. Natl. Acad. Sci. 117 (35), 21488–21494. https://doi.org/10.1073/pnas.2006024117.

Skovgaard, H., Carl, J.D., 2018. Restoration of Lake Lyng in Danish.

Sø, J.S., Sand-Jensen, K., Kragh, T., 2021. Optimal physical design in a new lake for reducing phosphorus pools. Ecol. Eng. 161, 106160. https://doi.org/10.1016/j.ecoleng.2021.106160.

Sorrell, B.K., Downes, M.T., Stanger, C.L., 2002. Methanotrophic bacteria and their activity on submerged aquatic macrophytes. Aquat. Bot. 72 (2), 107–119. https://doi.org/10.1016/S0304-3770(01)00215-7.

Striegl, R.G., Michmerhuizen, C.M., 1998. Hydrologic influence on methane and carbon dioxide dynamics at two north-central Minnesota lakes. Limnol. Oceanogr. 43 (7), 1519–1529. https://doi.org/10.4319/lo.1998.43.7.1519.

Tassi, F., Cabassi, J., Andrade, C., Callieri, C., Silva, C., Viveiros, F., Corno, G., Vaselli, O., Selmo, E., Gallorini, A., Ricci, A., Giannini, L., Cruz, J.V., 2018. Mechanisms regulating CO2 and CH4 dynamics in the Azorean volcanic lakes (São Miguel Island, Portugal): bio-geochemistry of volcanic lakes in the Azores,Portugal. J. Limnol. 77 (3). https://doi.org/10.4081/jlimnol.2018.1821.

Vachon, D., Prairie, Y.T., 2013. The ecosystem size and shape dependence of gas transfer velocity versus wind speed relationships in lakes. Can. J. Fish. Aquat. Sci. 70 (12), 1757–1764.

van Bergen, T.J., Barros, N., Mendonça, R., Aben, R.C., Althuizen, I.H., Huszar, V., Lamers, L.P., Lürling, M., Roland, F., Kosten, S., 2019. Seasonal and diel variation in greenhouse gas emissions from an urban pond and its major drivers. Limnol. Oceanogr. 64 (5), 2129–2139.

Varadharajan, C., Hemond, H.F., 2012. Time-series analysis of high-resolution ebullition fluxes from a stratified, freshwater lake. J.Geophys.Res.Biogeosci. 117 (G2).

Wik, M., Thornton, B.F., Bastviken, D., Uhlbäck, J., Crill, P.M., 2016. Biased sampling of methane release from northern lakes: a problem for extrapolation. Geophys. Res. Lett. 43 (3), 1256–1262.

Zhang, M., Xiao, Q., Zhang, Z., Gao, Y., Zhao, J., Pu, Y., Wang, W., Xiao, W., Liu, S., Lee, X., 2019. Methane flux dynamics in a submerged aquatic vegetation zone in a subtropical lake. Sci. Total Environ. 672, 400–409. https://doi.org/10.1016/j.scitotenv.2019.03.466.